Configurations of misfit dislocations at interfaces of lattice-matched $Ga_{0.5}In_{0.5}P$/GaAs heterostructures

Y. Q. Wang and Z. L. Wang[a)]
School of Materials Science and Engineering, Georgia Institute of Technology, Atlanta, Georgia 30332-0245

T. Brown, A. Brown, and G. May
School of Electrical and Computer Engineering, Georgia Institute of Technology, Atlanta, Georgia 30332

(Received 25 February 2000; accepted for publication 17 May 2000)

A configuration of misfit dislocation dipoles is observed in a $Ga_{0.5}In_{0.5}P$ heterostructure grown by solid-source molecular-beam epitaxy on GaAs. The dipole dislocations are mostly of 60° type, separated by ~3.5 nm. The dislocations are not produced by conventional lattice mismatch, rather, they could be the result of lateral compositional modulation in the $Ga_{0.5}In_{0.5}P$ epilayer. © *2000 American Institute of Physics.* [S0003-6951(00)02528-6]

Dislocations are the most frequently observed crystal defects in epitaxial semiconductor heterostructures.[1] Geometrically, they are generally categorized as threading and misfit dislocations. A threading dislocation, taking its line direction approximately parallel to the growth direction essentially makes no contribution to relaxation of the misfit strain that may possibly be present at the interface. In homoepitaxy and lattice-matched epitaxy, it has been shown that threading dislocations are replicated into the epilayers from the substrate.[2] Therefore, the dislocation density in the epilayer is principally determined by that of the substrate. Misfit dislocations are generated during the epitaxial growth and they are common features for lattice mismatched epitaxial films. In most cases, threading dislocations are concomitantly generated with misfit dislocations.[3,4] It has been well established that dislocations considerably influence the electronic and optical properties of semiconductor heterostructures and device performance.[5–7] The way in which misfit dislocations are introduced is intimately related with the actual epitaxial growth mechanism.[7–15] Therefore, study of dislocations is an important field in molecular-beam epitaxy (MBE) grown heterostructures.

It is generally believed that misfit dislocations will not be introduced until a critical epilayer thickness is reached, at which formation of misfit dislocations is favorable as compared with elastic accommodation of the misfit strain.[16] The linear misfit dislocation density is, to the first order approximation, proportional to the magnitude of misfit strain. It can be inferred that no misfit dislocation will be introduced if the misfit strain is negligibly small. Therefore, the major line defects are generally threading dislocations in homoepitaxial and lattice matched heteroepitaxial structure although other kinds of lattice defects can also be introduced under some particular conditions.[17,18] In this letter, we report a misfit dislocation array: dislocation dipoles, observed in the lattice-matched GaInP/GaAs heterostructure grown by the solid source molecular beam epitaxy. The introduction of this dislocation dipole configuration is considered to be associated with the lateral composition modulation in the GaInP epilayer.

The lattice matched GaAs/GaInP structures were grown on (001) GaAs wafers at a rate of ~1 μm/h in a standard three-chamber Riber MBE system with solid source effusion cells using As_4 as the arsenic species. The whole structure consists of about nine layers. In this study, we focus only on the interface of the GaAs buffer and the GaInP barrier layer, so only the growth conditions for these layers are given here. A 200 nm thick GaAs buffer was grown at 873 K with an As beam equivalent pressure (BEP) of 6×10^{-6} Torr. A 40 nm thick GaInP layer was grown at 793 K with P-BEP of 5×10^{-6} Torr. Electron microscopy analysis was carried out at 400 kV using a JEOL 4000 EX and at 200 kV using a Hitachi HF-2000.

Figure 1 shows TEM images of GaInP layer on GaAs

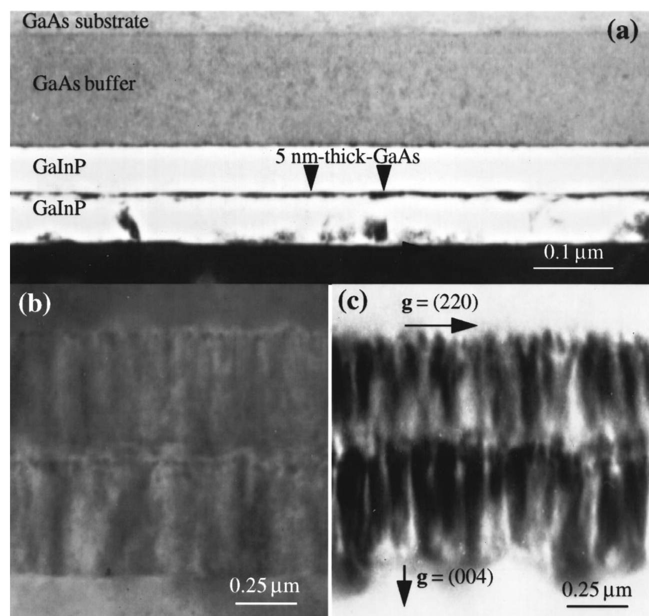

FIG. 1. Cross-sectional TEM images of the GaInP–GaAs heterostructure. (a) The (002) DFI showing different overlayers (GaInP: bright; GaAs: dark gray); (b) multibeam BFI and (c) the (220) DFI showing the contrast modulation in the GaInP overlayers.

a)Author to whom correspondence should be addressed; electronic mail: zhong.wang@mse.gatech.edu

 © 2000 American Institute of Physics
Downloaded 12 May 2004 to 130.207.165.29. Redistribution subject to AIP license or copyright, see http://apl.aip.org/apl/copyright.jsp

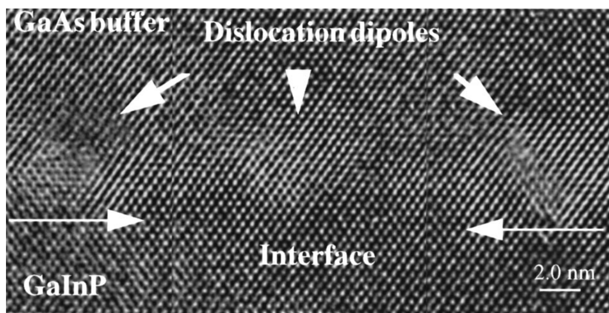

FIG. 2. HRTEM image showing dislocation dipoles distributing along the lattice matched interface between the GaAs buffer and GaInP epilayer.

buffer layer under different imaging conditions. The first two GaInP epilayers with a 5-nm-thick-GaAs layer are shown in the images. The composition-sensitive (002) dark field image (DFI) shows a well-defined interface between the GaInP overlayer and GaAs buffer [Fig. 1(a)]. No significant undulations have been observed along the interface. Interestingly, the interface between GaAs buffer and GaAs substrate can also be revealed by the DFI. Figure 1(b) is a bright field image (BFI) by using seven beams. Although the GaInP overlayers show a uniform contrast in the DFI, some fine contrast modulation normal to the growth direction can be seen. When the interface is inclined and imaged under two-beam conditions, the contrast modulation can be revealed more clearly, as shown in Fig. 1(c) which is a (220) BFI. The contrast modulates with a period of about 12.0 nm. A comprehensive analysis indicates that this contrast modulation is due to the lateral compositional modulation in the GaInP overlayer.[19]

Figure 2 is a HRTEM image of the interface between GaInP overlayer and GaAs buffer. It can be seen that there are a number of misfit dislocations distributed along the interface, although the GaInP overlayer has been expected to be lattice matched to the GaAs substrate (lattice constant: 0.5653 nm). However, no obvious increase in threading dislocation density has been observed. As compared to that of conventional misfit dislocations present in the lattice-mismatched heterostructures, the dislocations appear in pairs with opposite signs, forming a special configuration–dislocation dipoles. The distance between the dislocation dipoles averages ~3.5 nm. The dislocations are not exactly located at the interface. They are actually distributed in a zone of 3–5 nm in width in the GaInP epilayer. Furthermore, the distribution of the dislocations along the interface is not uniform. Lengths of up to several tens of nanometers are often dislocation free.

Based on the geometry of the dislocation dipoles, they are classified into three types: null, extrinsic, and intrinsic. When the two dislocations are aligned vertically above one another, they will combine and annihilate each other. We call this type to be the null-type dislocation dipole, as shown in Fig. 3(a). If the two extra half planes associated with the dipole dislocations overlap and combine into a new extra half plane, the dislocation dipole is extrinsic [see Fig. 3(b)]. Otherwise, it is called intrinsic [Fig. 3(c)]. It should be noted that the screw components are not taken into consideration in the above classification although the dipole dislocations are mostly of 60° type. Lomer dislocations have also been observed, as illustrated in Fig. 3(d). Formation of these three types of dislocation dipoles seems to be nonequally probable. In a total of 50 dislocation dipoles we observed, about 50% are extrinsic, 30% are null, and the rest are intrinsic.

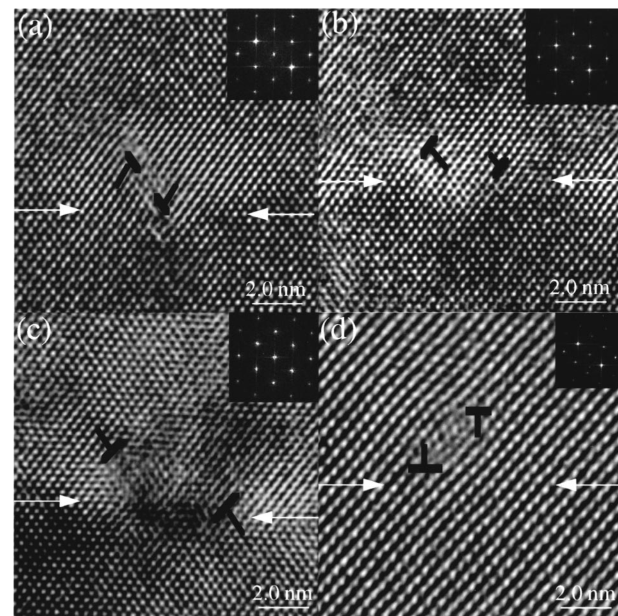

FIG. 3. Typical misfit dislocation dipole configurations: (a) extrinsic, (b) intrinsic, (c) null (d). The arrows indicate the interface position. The inset is the Fourier transform of the dislocation dipole areas.

A dislocation dipole basically has no long-range strain field. However, there exists strong interaction between its two dislocations, which can be described quantitatively in terms of the force acting on them. Assuming the material is isotropic, the interacting force in the direction of $\mathbf{b}_\perp$ between the two parallel 60° dislocations can be written as[20]

$$F=-\frac{G b_\perp^2}{2\pi(1-\nu)}\frac{1}{r}\cos\theta\cos 2\theta \pm \frac{G b_\parallel^2}{2\pi}\frac{1}{r}\cos\theta,$$

where the first term on the right-hand side of the equation represents the force between the two edge components and the second between the two screw components. The plus sign is chosen for the screw components of the same sign and the minus sign for the opposite signs. r is the distance between the two dipole dislocations and θ is the angle between the distance vector $\mathbf{r}$ and the Burgers vector of the edge component, as shown in Fig. 4(a). In the case where there is no external stress, the stable relative position of the two dislocations is determined by setting $F=0$. For the special case of two pure edges of the opposite sign, e.g., two Lomer dislocations, θ is found to be 45°. Considering that $0.5>\nu>0$, there is correspondingly a limiting range over which θ can vary, i.e., $35°<\theta<40°$ or $50°<\theta<55°$. The predicted stable arrays of the dislocation dipoles are shown in Fig. 4. In principle, the θ angle can be used to determine the Burgers vectors $\mathbf{b}_1$ and $\mathbf{b}_2$ of the two dipole dislocations. If $\theta>45°$, the two screw components have the same sign. They repel each other and tend to separate the two 60° dislocations. The Burgers vectors of the two dipole dislocations will be $a/2[\bar{1}01]$ and $a/2[0\bar{1}1]$, respectively. Alternatively, $\theta<45°$ indicates that the two screw components attract each other, hence the two 60° dislocations are of opposite sign.

Downloaded 12 May 2004 to 130.207.165.29. Redistribution subject to AIP license or copyright, see http://apl.aip.org/apl/copyright.jsp

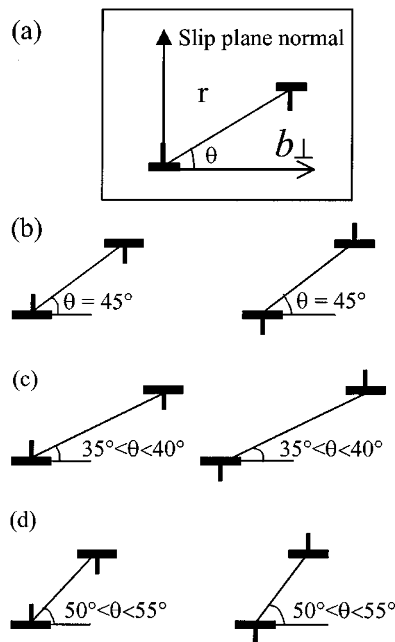

FIG. 4. Relative stable positions of two opposite dislocations in a dislocation dipole. Left-hand side column: extrinsic type; right-hand side column: intrinsic type.

Our measurement shows that the distance r between the two dislocations is ~3.5 nm and the angle θ is ~15° or 75° for both extrinsic and intrinsic dislocation dipoles. Obviously, the θ value is not within the range for the stable configuration. The large discrepancy in θ between the experimental value and the theoretical prediction is considered to result from the presence of high local stress field, which is evidenced by the considerable local lattice distortions in the HRTEM images. This viewpoint is further supported by the presence of the null-type dislocation dipoles. In this case, $\theta = 0$, the interacting force is always attractive (negative) and is inversely proportional to the distance r, no matter whether the two 60° dislocations have like or dislike screw components. Therefore, the two 60° dislocations tend to combine with each other, resulting in a complete annihilation of the dislike screw components or a pure screw with a Burgers vector of $2b \cos 60°$ for like screw components. These combinations are apparently favored energetically. However, we have observed frequently that the two 60° dislocations are separated by ~1.5 nm, implying that there must be an opposing force to prevent them from combination.

Dislocation dipoles are common microstructure features of plastically deformed metals and constitute the basis for the theory of short-range work hardening.[21] There are several mechanisms that have been proposed for the formation of dislocation dipoles.[22] However, all these mechanisms necessitate the preexistence of dislocations and involve considerable movement and interaction of dislocations, and they are considered unlikely to operate in the present case. Jain *et al.* analyzed the dislocation arrays in a capped strained epilayer.[23,24] They point out that if the cap layer is sufficiently thick, relaxation of the misfit strain occurs by introduction of dislocation dipoles, one dipole dislocation being at the upper interface and the other at the lower interface. The location of dislocation dipoles in their case is apparently different from ours. We believe that formation of the three types of dislocation dipoles must be related to compositional modulation occurring in the GaInP overlayers. Compositional modulation brings the single uniform GaInP phase decomposed into two phases that have the same crystal structure but different compositions, one of which is Ga rich and the other is In rich. Due to the atomic size difference, the (Ga-rich) phase or regions experience tensile stress while the In-rich regions experience compressive stress to match the GaAs substrate. Furthermore, the Ga-rich regions also need to match the In regions. When the mismatch at these regions reaches a critical value, dislocations need to be introduced to relax the misfit strain. Considering that the dislocation density is very low in the substrate and no obvious increase of threading dislocations is observed, the formation of dislocation dipoles cannot be accounted for solely in terms of the Matthews model,[25] in which misfit dislocations are formed by bending the treading dislocations into the interface.

The authors gratefully acknowledge the support from the Air Force Research Laboratory under Contract No. F33615-98-C-5428, and the Georgia Institute of Technology Molecular Design Institute, under Prime Contract No. N00014-95-116 from the Office of Naval Research.

[1] D. W. Pashley, Mater. Sci. Eng. **15**, 2 (1999).
[2] E. A. Beam III, S. Mahajan, and W. A. Bonner, Mater. Sci. Eng., B **7**, 83 (1990).
[3] N. A. El-Masry, J. C. Tam, and N. H. Caram, J. Appl. Phys. **64**, 3672 (1988).
[4] W. Qian, M. Skowronski, R. Kaspi, and M. De Graef, J. Appl. Phys. **81**, 7268 (1996).
[5] J. P. R. David, Y. H. Chen, R. Grey, G. Hill, P. N. Robinson, and P. Kightley, Appl. Phys. Lett. **67**, 906 (1995).
[6] R. K. Jain and D. J. Flood, IEEE Trans. Electron Devices **40**, 1928 (1993).
[7] M. Meshkinpour, M. S. Goorsky, and G. Chu, Appl. Phys. Lett. **66**, 748 (1995).
[8] A. Vila, A. Cornet, J. R. Morante, P. Ruterana, M. Loubradou, and R. Bonnet, J. Appl. Phys. **79**, 676 (1996).
[9] J. Zou, D. J. H. Cockayne, and J. J. Russell-Harriott, Appl. Phys. Lett. **70**, 3134 (1997).
[10] A. G. Cullis, A. J. Pidduck, and M. T. Emeny, Phys. Rev. Lett. **75**, 2368 (1995).
[11] A. Lefebvre and C. Ulhaq-Bouillet, Philos. Mag. A **70**, 999 (1994).
[12] J. Narayan and S. Sharan, Mater. Sci. Eng., B **10**, 261 (1991).
[13] V. I. Vdovin, Phys. Status Solidi A **171**, 239 (1999).
[14] B. Pichaud, M. Putero, and N. Burle, Phys. Status Solidi A **171**, 251 (1999).
[15] S. C. Jain, A. H. Harker, and R. A. Cowley, Philos. Mag. A **75**, 1461 (1997).
[16] J. W. Matthews and A. E. Blakeslee, J. Cryst. Growth **27**, 118 (1974); **29**, 273 (1975); **32**, 265 (1976).
[17] B. V. Dutt, S. Mahajan, R. J. Roedel, G. P. Schwartz, D. C. Zmiller, and L. Derick, J. Electrochem. Soc. **128**, 1573 (1981).
[18] J. Vanhellemont, J. De Boeck, G. Borghs, and R. Mertens, Inst. Phys. Conf. Ser. **100**, 109 (1989).
[19] Y. Q. Wang, Z. L. Wang, T. Brown, A. Brown, and G. May (unpublished).
[20] D. Hull and D. J. Bacon, *Introduction to Dislocations*, 3rd ed. (Pergamon, Oxford, 1984), p. 83.
[21] J. J. Gilman, J. Appl. Phys. **33**, 2703 (1962).
[22] *Physical Metallurgy*, 4th ed., edited by R. W. Cahn and P. Haasen (North-Holland, Amsterdam, 1996), Vol. 3, p. 2307.
[23] S. C. Jain, T. J. Gosling, J. R. Willis, R. Bullough, and P. Balk, Solid-State Electron. **35**, 1073 (1992).
[24] J. R. Willis, S. C. Jain, and R. Bullough, Philos. Mag. A **64**, 629 (1991).
[25] J. W. Matthews, Philos. Mag. **13**, 1207 (1966).

Downloaded 12 May 2004 to 130.207.165.29. Redistribution subject to AIP license or copyright, see http://apl.aip.org/apl/copyright.jsp